# Dosimetry in small x-ray fields

Author: Laura Iscla Murria.

Advisor: Dr. José M. Fernández-Varea.
*Facultat de Física, Universitat de Barcelona, Martí i Franqués 1, 08028 Barcelona, Catalonia*.*

**Abstract**: In this work we study the behaviour of small x-ray fields in radiotherapy, whose dosimetry presents a number of problems. The study requires learning how to use the penEasy program. The analysis consists on measure the absorbed dose according to the field size. The study allows us to discuss some graphical representations of the data computed and compare them with experimental values taken with an Exradin W1 Scintillator.

## I. INTRODUCTION

Radiotherapy treatments are intended to supply a prescribed absorbed dose to the cancer cells while trying to not harm healthy tissue. Nowadays small photons fields are often used in radiotherapy. Progress in diagnostic techniques has led to an early diagnosis. Thus, the size of the tumours to be treated has decreased. In addition, modern therapy equipment allows the conformation of very small fields. Both reasons have increased the need to characterize dosimetrically fields smaller than 4x4 $cm^2$. The dosimetry of these small fields presents some problems due to the size and occlusion of the source, the lack of electronic equilibrium and perturbations that the detector introduces.

The source occlusion produces a rise in the penumbra when we reduce the field size. In contrast with large fields in which we have a constant and stable dose, when the detector can only see part of the x-ray source, the output will be smaller than it is supposed to be without occlusion. The results bring uncertainties in the FWHM (full width at half maximum) determination. As a consequence, we obtain overestimated values. The lack of electronic equilibrium is related to the presence of the secondary electrons, it depends on the beam energy and increases the penumbra ranges for small fields [1, 2].

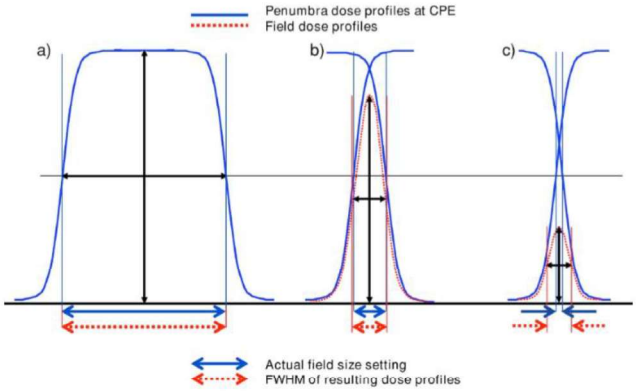


**FIG. 1**: Comparation between FWHM for different field size. (a) Big field size with FWHM correctly calculated. (b) Small error caused by the FWHM determination. (c) Overestimated field size. CPE= charged particle equilibrium. Figure taken from reference [1].

Last but not least, the physical dimensions of the detector introduced can perturb the measurements because some detectors are not as small as required if we compare them with the field dimensions. As a consequence, it is a challenge to choose the best detector.

With the objective of studying the dose distribution in small fields for 6 MV and 15 MV photon beams, in this project we will compare the experimental output factors with Monte Carlo simulations performed with the PENELOPE/penEasy program.

## II. MONTE CARLO SIMULATIONS

PENELOPE is a code for the Monte Carlo simulation of coupled electron/photon transport. The programme is based on the generation of random showers in materials of arbitrary composition. The simulations can follow in detail the trajectories of the generated electrons and photons [2]. PENELOPE has been extensively used in medical physics, to do simulation in dosimetry, radiological protection, radiotherapy and nuclear medicine.

In order to run a simulation with penEasy we need to create (at least) three files: the geometry, the material and the input file.

### A. Geometry

With the interest of achieving a certain geometry according to our preferences we must define analytical functions whose purpose is to describe the different surfaces. We start choosing the reduced form of this analytical expression is given by [4].

$$F_r(r) = I_1x^2 + I_2y^2 + I_3z^2 + I_4z + I_5 \qquad (1)$$

whose coefficients can take the values of -1, 0 or 1. This includes planes, spheres, cylinders, ellipsoids, etc. Next, it may be necessary to scale, rotate and displace equation (1). These parameters are included in the geometry file.

Once a certain number of surfaces have been defined, we use them to delimit bodies. Bodies can also be delimited by previously defined bodies. They have to be defined in ascending order. So, if one body is inside another, the second body must be delimited by its corresponding surfaces and the first body in order to not overlap [3,4].

The created geometry is composed by 11 surfaces and 4 bodies. It consists of a 50x50x50 $cm^3$ water phantom and a cylindrical polystyrene dosimeter on the $z$ axis.

* Electronic address: laura.iscla@gmail.com

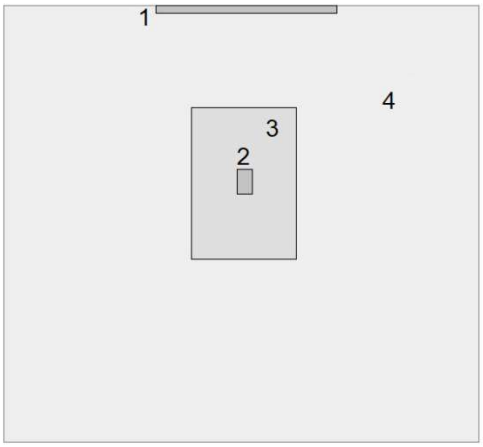


**FIG. 2**: Geometry of the file used in the PENELOPE simulations. (1) Is the square field geometry, whose dimension varies for each simulation. (2) Refers to the scintillating detector. (3) Is the auxiliary body. (4) Is the water container with dimensions of 50 cm each side.

The field sizes used were square fields between 0.5 cm and 3.5cm. The auxiliary body is a cylinder with 1 cm diameter, it has been created with the purpose of reducing the simulation time. It is made with the same material as the container. The auxiliary body has a different energy limit of existing particles than the other surfaces in order to have a quicker simulation with a higher number of particles.

### B. Materials

By designing the simulation, it is possible to choose the material of each body. The first body, the field, whose dimensions vary conveniently has been made with water. As well as, the auxiliary body and the main tank.

On the contrary, the detector, which reproduces a scintillator, is made of polystyrene ($C_8H_8$) because we want a simulation that can be as similar as possible to reality. The polystyrene material file has been created from the list of possible materials that the that the auxiliary program material.exe includes. Which reads the interaction cross sections of the PENELOPE data base.

### C. Input files

The input file is the one used to run the program and it links the geometry and material file(s). It is the one used to run the program and it groups the geometry and material file. By editing the input file, we can set the characteristic of the beam, namely type of particle, energy spectrum, initial position and direction. The electron and photon absorption energy in each body were set at $10^5$ eV for electrons and positrons at the detector and the auxiliary body, $10^6$ eV at the field and the water tank and $10^4$ eV for photons in all bodies. The number of particles chosen for the simulation was at least $10^8$ in order to achieve good statistics. Furthermore, the input file is also used to activate tallies and set other characteristics of the output according to the purpose of each simulation.

## III. PERFORMED SIMULATIONS

Different simulations were performed according to the output that we wanted. To obtain the desired data we need to activate the relevant tally section. The "energy deposition" tally was activated to determine $TPR_{20,10}$ index.

With the objective of having a simulation as accurate as possible, the spectra used in the simulation are the corresponding to the Varian linear accelerator of the hospital provided by *Sheikh-Bagheri and Rogers,* and done with Monte Carlo calculation [5].

To compare the different spectra, we need to define the $TPR_{20,10}$ index. The $TPR_{20,10}$ refers to the beam quality, it is the ratio between the absorbed dose at 20 cm and 10 cm of deepness. With the aim of calculating the $TPR_{20,10}$ the field size set was 10x10 $cm^2$ at the depth where the detector is placed.

$$TPR_{20,10} = \frac{D_{20cm}}{D_{10cm}} \quad (2)$$

The main advantage of the $TPR_{20,10}$ index is that it does not depend on the electron contamination of the incoming beam. And also, little setting effects do not affect the result because we are doing a ratio. To calculate the $TPR_{20,10}$ of each beam we use the geometry displayed in figure 3. By running the simulation twice for each energy (one with at 10 cm and another at 20 cm) we can evaluate the $TPR_{20,10}$ [6].

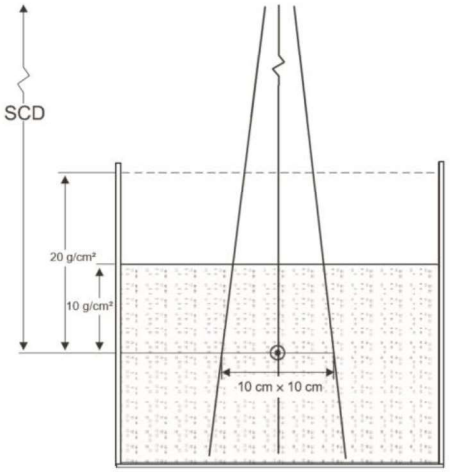


**FIG. 3**: Geometry used to calculate the $TPR_{20,10}$ index where SCD refers to the distance between the source and the detector and it remains constant during both simulations (at 10 cm and at 20 cm). Figure taken from reference [6].

Also, several simulations comparing the absorbed dose in water (that is, without the detector) or in the polystyrene detector according to field size or depth were performed. For those in water we need to activate the "cylindrical dose distribution" tally and for the detector ones the "energy deposition" tally was activated.

## IV. EXPERIMENT

The results of the experimental data were obtained in the Hospital de la Santa Creu i Sant Pau of Barcelona during the internship period. The experimental data were taken using a Varian clinac 2100 C/D accelerator. The main parts of the linac are: gantry with the beam, first collimator, flattering filter, jaws, multi leaf, and the treatment table. The field sizes were delimeted using only jaws, and also using both the jaws and the multi leaf collimator (MLC).

6 MV and 15 MV photon beams delivered by the linear accelerator were used during the experiment. The $TPR_{20,10}$ index of these beams is 0.6657 and 0.7607, respectively. Also, we used 100 MU (monitor units). Monitor unit is a form of measuring the machine output. Frequently 100 MU correspond to 1 Gy of absorbed dose at 100 cm source distance, but the actual value depends on the accelerator calibration.

The simulations were set up with the same conditions as the experimental assembly to compare both results. The experimental scintillator detector used was Exradin W1 Scintillator. This dosimeter is affected by Cherenkov radiation, which is electromagnetic radiation produced by charged particles with velocities higher than the speed of light in a given medium. The scintillator has two output channels, each one refers to a different voltage treated with the following method in order to eliminate the Cherenkov contribution.

$$Dose = Gain\ (SC1 - SC2 \cdot CLR) \tag{3}$$

where SC1 and SC2 refer to the two output channels. CLR (Cherenkov light radiation) and Gain were calibrated during the experiment.

Besides, neither the simulation nor the experimental data are not reported as absorbed dose. It is customary to define the output factor (OF) that refers to the normalization of the dose with respect to a reference field.

$$OF_i = \frac{D_i}{D_{ref}} \tag{4}$$

Generally, a 10x10 $cm^2$ field is used in the normalization of OF although it would also be valid for small fields to use a 3.5x3.5 $cm^2$ field.

With the aim of obtaining valid experimental data several corrections need to be applied to the raw data.

### A. Cherenkov correction

Knowing that the scintillator is perturbed by the Cherenkov light we have to introduce a correction in the CLR and Gain values. These values will determine the final absorbed dose in the scintillator.

The correction values for the Cherenkov radiation were developed with a 3.5x3.5 $cm^2$ reference field in the normalization of the output factor.

**TABLE I**: Corrected values of the Cherenkov correction applied in experimental data.

| | 6 MV | 15 MV |
|---|---|---|
| CLR | 0.749611 | 0.702475 |
| Gain | 0.037142 | 0.034099 |

### B. Field-size correction

The field size refers to the pair of dimensions that define the area of each measured field. Dimensions are defined by the FWHM of the lateral profile of the absorbed dose. Field size is used as irradiation field size. Initially, the experimental data were displaced with respect to those of the simulation because the dimensions of the field were not the real ones.

Due to the fact that the field size of experimental data is not as precise as needed they were corrected following the next procedure. This procedure considers the fact that experimental sizes are not accurate and realign the size values. Also, the linac MLC do not allow to perform very small square fields. On the contrary, fields on the order of 0.5x0.5 $cm^2$ are rectangular with dimensions of 0.5x1 $cm^2$.

According to the procedure used the normalizing procedure has been executed with:

$$S = \sqrt{AB} \tag{5}$$

This refers to the fact that for rectangular fields the geometric average of each side would be the final side length [7].

### C. Output Factor correction

Finally, the correction of the output factor has been obtained by measurements with an ionization chamber PTW30010 for a field of 3.5x3.5 $cm^2$ [7].

**TABLE II**: Correction values for the output factor applicable to an experimental field previously normalized to 3.5x3.5 $cm^2$.

| | OF | Uncertainty |
|---|---|---|
| 6 MV | 0.8445 | 0.0009 |
| 15 MV | 0.8886 | 0.0006 |

## V. RESULTS AND DISCUSSION

First of all, to discuss the photon spectra used in the simulation it is necessary to say that the spectra are idealized because positrons and electrons contamination is neglected. It can be seen in the Fig. 4 how the relative depth-dose curve (normalized to 100%) changes between a monoenergetic and a continuous spectrum. Unless both have the same energy, it can be easily seen how different the spectra are. Maximum point in the two spectra are not the same. The 6 MV monoenergetic spectrum has its maximum deeper than the continuous one. If the spectra were not normalized it would be possible to notice how the continuous one is lower while the monoenergetic is higher, this occurs because the energies in the continuous spectra is distribute along the spectra with a maximum around 2 MeV. With the purpose of doing realistic simulations we have choose the continuous x-ray spectra similar to the ones delivered by the linac.

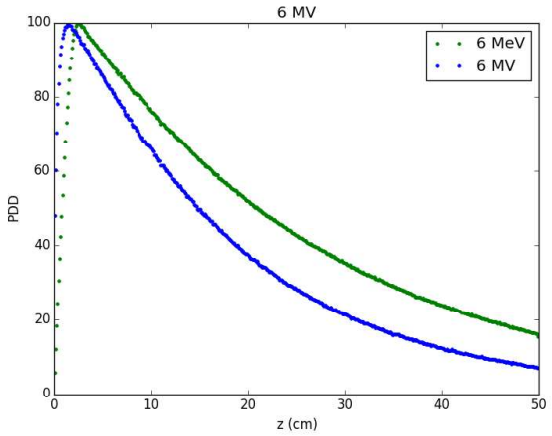


**FIG. 4**: Percentage depth-dose curves for a 6 MeV monoenergetic beam (green curve) and a continuous 6 MV spectrum (blue curve).

Now, we should discuss the quality of the beam we are using in the simulation. To do it, $TPR_{20,10}$ has been calculated with the method mentioned before. As we can see in Table 1 for different energies the value of the $TPR_{20,10}$ varies. But it changes also between several types of accelerators with the same energy. So, we will choose the one more similar to the hospital accelerator. Knowing that the $TRP_{20,10}$ of the hospital accelerator is 0.6657 for 6 MV and 0.7607 for 15 MV. We can say that the quality for our spectra (Varian 6 MV and 15 MV) are quite similar to the hospital ones. Notice how the $TPR_{20,10}$ varies between several types of machines with the same energy.

**TABLE III**: $TPR_{20,10}$ values calculated from Monte Carlo simulations for various energy spectra [5].

| Type | Energy (MV) | $TPR_{20,10}$ |
|---|---|---|
| Varian | 4 | 0,653±0,006 |
| Elekta | 6 | 0,716±0,006 |
| Siemens | 6 | 0,716±0,006 |
| Varian | 6 | **0,658±0,006** |
| Varian | 15 | **0,757±0,005** |
| Varian | 18 | 0,826±0,005 |

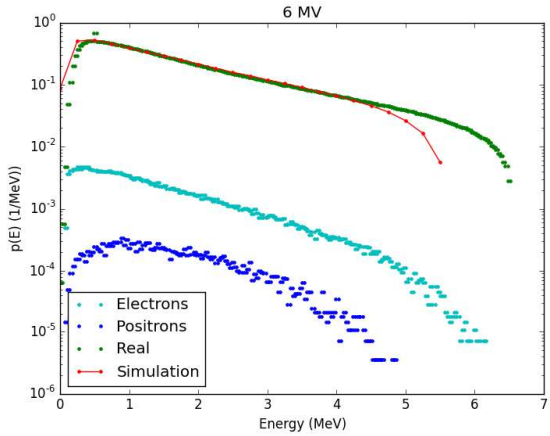


**FIG. 5**: Semilogarithmic plot of the simulated beam and the real beam with its electron and positron contamination [9].

In order to obtain a $TPR_{20,10}$ more similar to the hospital one it would be necessary to simulate the gantry of same model machine and adapt the initial beam energy with an iterative method [8]. However, the waveguide will not be exactly the same, and even a little difference introduces variations to the genereated beam. And this kind of simulation is well beyond the scope of the present work. Perhaps the beam used at the simulation is not perfect, in Fig5. it is possible to see that it is quite similar.

Measurements have been taken with the Exradin W1 Scintillator. Comparing the results for fields sizes between 0.5x0.5 $cm^2$ and 3.5x3.5 $cm^2$. We can observe that for square fields the output factor decreases quicker when they are delimited with only the linac jaws. This is due to the source occlusion effect caused when the jaws are too closed in order to project very small fields, and the absorbed dose therefore is lower.

The results for the MLC had been taken with the jaws forming a 3.5x3.5 $cm^2$ field size and the MLC delimiting the precise size needed in each case. This measurement departs from those of the simulation but with the correction factors introduced they fall within the limits of the error bars.

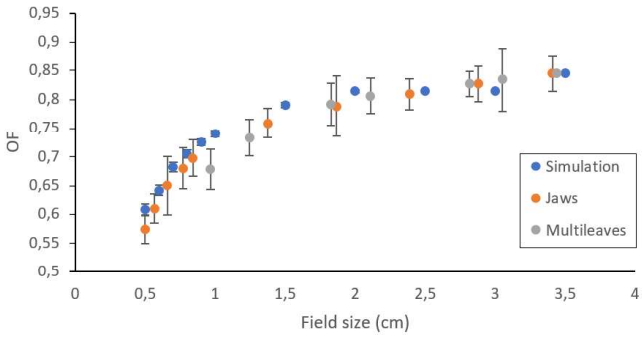


**FIG. 6**: OF as a function of field sizes for a 6 MV beam. Experimental data were obtained defining the fields either with the jaws or with the MLC.

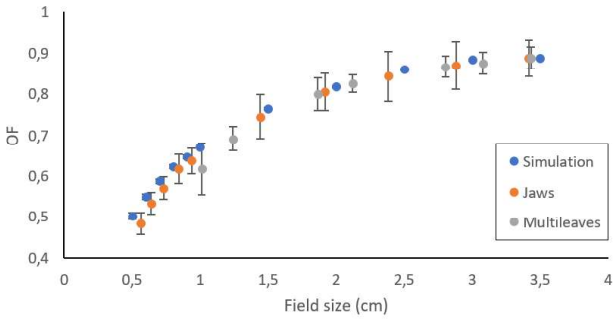


**FIG. 7**: OF as a function of field sizes for a 15 MV beam. Experimental data were obtained defining the fields either with the jaws or with the MLC.

By computing the absorbed dose at the detector for several depths between 0 and 20 cm we can compare the effects of the detector in the simulation. As we can see in Fig. 7 the simulations with and without the scintillator detector follow the same trend. The graphical representation of simulation with detector is a lot more noisy than the other one because the data had been taken point by point in each depth. It has to be

read as a guiding path of the behaviour of the dose in deepness with detector.

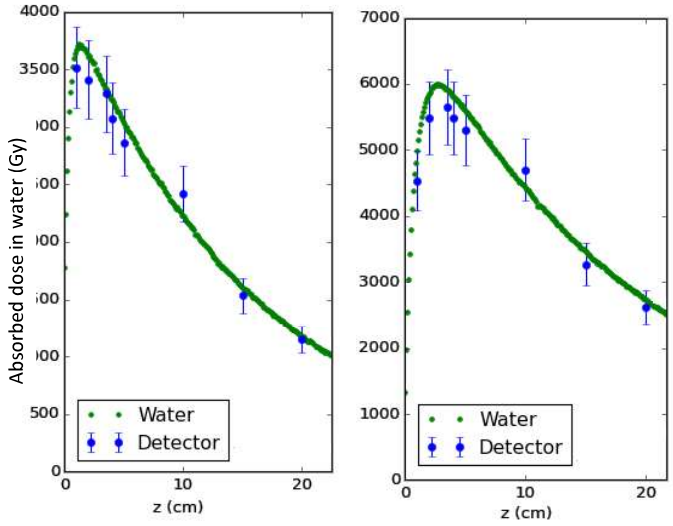


**FIG. 8**: Graphical view of dose in depth between simulations with and without detector for 6 MV (left) and 15 MV (right). The error bars correspond to one standard deviation. For MV beams, dose to water and dose to polystyrene are assumed to be identical.

Notice that the simulated depth-dose curves in the water phantom is too small very close to the surface. This is because in the simulation we did not included electron contamination.

## VI. CONCLUSIONS

Both the experimental and simulated measurements depending on the field size show the source occlusion effects as we expected. These effects have been found in the measurements done with jaws or the MLC delimiting the field size.

Monte Carlo simulation is a very useful method for the determination of absorbed dose in medical physics.

The $TPR_{20,\ 10}$ indexes of the different spectra show that although having the same nominal energy the spectra used in different machines are not the same. Furthermore, the experimental and simulated spectra are not identical; although both, the nominal energies and machine type are the same.

The simulation and the experimental OF are according to each other after having applied the three corrections.

The most relevant of the three corrections and the one that introduce the more valid values is the field size correction.

Unless the scintillator is a good detector for small fields it introduces little perturbations. It is worth it to say that finding the adequate detector for small fields can be very challenging because of its dimensions and the possible uncertainties introduced by the detector.

## Acknowledgments

I would like to thank my advisor Dr. José M. Fernández-Varea for guiding me during this process.

I would like to thank all the radiophysics team of the Hospital de la Santa Creu i Sant Pau for helping and teaching me how to take the experimental data and welcoming me during the internship period.

Finally, I am grateful to my family and friends for their support.

[1] I. Das, G. X. Ding and A. Ahnesjö *et al*. "Small fields: Nonequilibrium radiation dosimetry", *Med. Phys.* **35** (1) 206-215 (2008).

[2] ICRU, "Prescribing, Recording, and Reporting of Stereotactic Treatments with Small Photon Beams", *Journal of the ICRU,* **14** (2) (2014).

[3] F. Salvat. "The PENELOPE code system. Specific features and recent improvements", Joint International Conference on Supercomputing in Nuclear Applications and Monte Carlo 2013, Paris, 2013.

[4] F. Salvat. "PENELOPE-2014. A Code System for Monte Carlo Simulation of Electron and Photon Transport" (Issy-les_Moulineaux, OECD/NEA, 2015) chapters 1 and 7.

[5] D. Sheikh-Bagheri and D. W. O. Rogers. "Monte Carlo calculation of nine megavoltage photon beam spectra using the BEAM code", *Med. Phys.* **29** (3) 391-402 (2002).

[6] IAEA, "Determinación de la dosi absorbida en radioterapia con haces externos", TPR 398, ch. 6, Viena (2005).

[7] IAEA, "Dosimetry of small static fields used in external beam radiotherapy", chapters 3 and 6, Viena (2017).

[8] J. Pena *et al.* "Photon beams automatic comissioning in Monte Carlo simulation", *Med. Phys.* **34** (3) 1076-1084 (2007).

[9] J. M. Fernández-Varea *et al.* "Monte Carlo based water/medium stopping-power ratios for various ICRP and ICRU tissues", *Phys. Med. Biol.* **52** 6475-6483 (2007).